


# Spinal NF- $\kappa$ B upregulation contributes to hyperalgesia in a rat model of advanced osteoarthritis

Yunze Li<sup>1,2</sup> , Yixin Yang<sup>2</sup>, Jinwan Guo<sup>3</sup>, Xuejiao Guo<sup>2</sup>, Zhiying Feng<sup>2</sup>  and Xuli Zhao<sup>1</sup>

Molecular Pain  
Volume 16: 1–12  
© The Author(s) 2020  
Article reuse guidelines:  
sagepub.com/journals-permissions  
DOI: 10.1177/1744806920905691  
journals.sagepub.com/home/mpx  


## Abstract

Knee osteoarthritis (OA) pain is the most common joint pain. Currently, dysfunction in the central nervous system rather than knee joint degeneration is considered to be the major cause of chronic knee OA pain; however, the underlying mechanism remains unknown. The aim of this study was to explore whether spinal NF- $\kappa$ B plays a critical role in chronic knee OA pain. In this study, we used a model induced by the intra-articular injection of monosodium iodoacetate. Spinal NF- $\kappa$ B and the phosphorylation and activation status of NF- $\kappa$ B p65/RelA (p-p65) were inhibited by the intrathecal injection of the inhibitor pyrrolidine dithiocarbamate in this model. After behavioral assessment, the knee was dissected for histopathology, and the spinal cord was dissected and examined for NF- $\kappa$ B, p-p65, and cytokine expression. Furthermore, the quantity and activity of neurons, astrocytes, and microglial cells and their colocalization with p-p65 in the spinal dorsal horn were investigated. Our findings included the following: (1) histology, the pathological changes in the joints of the knee OA model were basically consistent with knee OA patients; (2) the protein and transcription levels of NF- $\kappa$ B/p65 and p-p65 increased before day 14, appeared to decrease on day 21 and increased again on day 28, and the tendency of weight bearing was similar; (3) on days 21 and 28, the intrathecal injection of pyrrolidine dithiocarbamate markedly prevented the monosodium iodoacetate-induced reduction in the paw withdrawal threshold; (4) real-time polymerase chain reaction demonstrated that the expression of TNF- $\alpha$  and IL-33 was suppressed in the knee OA model by the intrathecal injection of pyrrolidine dithiocarbamate; and (5) immunofluorescence revealed that astrocytes were activated and that p-p65 was mainly increased in astrocytes. Our findings indicate that the spinal NF- $\kappa$ B/p65 pathway in astrocytes modulates neuroimmunity in rat model of intra-articular monosodium iodoacetate-induced advanced OA.

## Keywords

Osteoarthritis, chronic pain, NF- $\kappa$ B/p65, astrocyte

Date Received: 16 July 2019; Revised 10 December 2019; accepted: 3 January 2020

## Introduction

Knee osteoarthritis (OA) is the most common joint disorder, and its incidence is rising worldwide.<sup>1</sup> The global age-standardized prevalence of knee OA is 3.8%.<sup>2</sup> The overall prevalence of symptomatic knee OA is 8.1% and increases with age in China.<sup>3</sup> Although many nonsurgical treatments, including self-management, physiotherapeutic management, and drug therapy, are available, none are considered ideal for alleviating knee OA pain.<sup>4</sup> Moreover, some patients develop advanced knee OA pain characterized by ongoing pain that persists during rest and is resistant to nonsteroidal anti-inflammatory drugs. A total of 16%–39% of the knee OA patients still have chronic pain six months after

<sup>1</sup>Department of Pain Medicine, Shandong Provincial Hospital Affiliated to Shandong First Medical University, Jinan, China

<sup>2</sup>Department of Pain Medicine, The First Affiliated Hospital, Zhejiang University School of Medicine, Hangzhou, China

<sup>3</sup>Department of Anesthesiology, Shandong Provincial Qianfoshan Hospital, Jinan, China

### Corresponding Authors:

Xuli Zhao, Department of Pain Medicine, Shandong Provincial Hospital Affiliated to Shandong First Medical University, 324 Jingwu Road, Jinan, Shandong 250021, China.

Email: dizzyzhaoxl@163.com

Zhiying Feng, Department of Anesthesiology and Pain Medicine, The First Affiliated Hospital, Zhejiang University School of Medicine, Hangzhou 310003, China.

Email: fzy1972@zju.edu.cn



total knee replacement (TKR) surgery.<sup>5</sup> Chronic advanced OA pain causes severe physical and mental suffering.<sup>6</sup> Thus, there is a need to understand the underlying mechanisms of advanced OA pain to guide the development of improved therapies.

Clinical and experimental studies have provided evidence that pain intensity is not consistent with the change in the joints of patients with advanced OA pain.<sup>7</sup> Despite moderate to severe pain, patients with advanced OA pain have symptoms and signs of central sensitization, such as widespread pain, low pressure pain, and enhanced temporal summation.<sup>8</sup> Furthermore, based on the effect of treatment with neuropathic pain drugs, chronic OA pain involves central sensitization.<sup>9</sup> Experiments have also revealed features of central sensitization in an advanced OA model.<sup>7</sup> After intra-articular MIA injection, rats exhibit enhanced spinal response to mechanical stimulation of the paw skin.<sup>10</sup> However, the mechanisms of central sensitization in advanced knee OA are poorly understood.<sup>11</sup>

Proinflammatory cytokines such as IL-1 $\beta$ , IL-6, and TNF- $\alpha$  are key mediators of joints in human and experimental OA and are mainly produced by chondrocytes, synoviocytes, and macrophages.<sup>12–14</sup> Im et al. found significant increases in the concentrations of IL-1 $\alpha$ , IL-1 $\beta$ , TNF- $\alpha$ , IL-17, RANTES, and other inflammatory mediators in the lumbar spinal cord in the MIA model.<sup>15</sup> Moreover, it is well demonstrated that proinflammatory cytokines are involved in the central mechanisms of hyperalgesia.<sup>16</sup>

Nuclear factor- $\kappa$ B (NF- $\kappa$ B), a transcription factor for many cytokines, including IL-1 $\beta$ , IL-6, and TNF- $\alpha$ , has been suggested to be important for the generation of nociceptive sensitization and central sensitization induced by nerve injury, paclitaxel, etc.<sup>17–19</sup> The NF- $\kappa$ B p50/p65 heterodimer, the most common and best-characterized form, plays an important role in the regulation of gene expression in the central nervous system.<sup>20</sup> The complex regulation of NF- $\kappa$ B function in pathological conditions, in particular phosphorylation, is more worthy of our attention than the regulation of its physiological function.<sup>21</sup> Phosphorylation plays a critical role in NF- $\kappa$ B activation downstream of a variety of stimuli, from immune receptors to cytokines and growth factor receptors. NF- $\kappa$ B phosphorylation controls transcription in a gene-specific manner, providing a new opportunity to selectively target NF- $\kappa$ B to achieve therapeutic goals.<sup>22,23</sup>

A previous study demonstrated that the inhibition of NF- $\kappa$ B/p65 reduces mechanical and thermal hyperalgesia following peripheral nerve injury.<sup>24</sup> The findings of our recent study showed that the intrathecal injection of a lentiviral vector, LV-sh NF- $\kappa$ B/p65, knocks down the expression of NF- $\kappa$ B/p65 and significantly attenuates hyperalgesia, paw edema, and joint destruction

following treatment with Freund's complete adjuvant.<sup>25</sup> These findings suggest that NF- $\kappa$ B/p65 plays a role in central sensitization. However, whether spinal NF- $\kappa$ B/p65 can also facilitate advanced knee OA pain has not been well investigated. Therefore, we determined whether the inhibition of spinal NF- $\kappa$ B/p65 expression can significantly influence advanced knee OA pain.

Using a rat model of advanced OA pain, we tested the following hypotheses: (1) NF- $\kappa$ B/p65 increases in the spinal cord of an advanced knee OA pain model and (2) pyrrolidine dithiocarbamate (PDTC), a NF- $\kappa$ B inhibitor, blocks advanced knee OA pain by downregulating proinflammatory cytokines.

## Materials and methods

### Animals

Adult male Sprague-Dawley rats weighing 250 to 300 g were purchased from the Laboratory Animal Center of Shandong University. The animals were housed in a controlled environment (temperature of 22°C–23°C, relative humidity of 40%–60%, 12-h light/dark cycle, lights on at 8 a.m.) with standard diet and water available ad libitum. All rats were allowed to habituate to the animal facility for at least one week prior to experimentation. All experimental protocols and procedures were approved by the Animal Care and Use Committee of Shandong Provincial Hospital affiliated with Shandong University. The guidelines of the Committee for Research and Ethical Issues of International Association for the Study of Pain were followed.

### Model of knee OA

A knee osteoarthritis model was established according to a previously described procedure.<sup>26</sup> MIA (Sigma, USA) was dissolved in normal saline (NS) to a final concentration of 80 mg/ml. Briefly, under 10% chloral hydrate (330 mg/kg, i.p.) anesthesia, the right hind leg of each rat was shaved around the knee with minimal wounds. The knee capsule was identified by palpating the patella and tibial plateau, and the injection was delivered by advancing a 25-gauge needle through the skin and patellar ligament to the anterolateral border of the tibial plateau until it entered the joint capsule. Then, 60  $\mu$ l MIA (80 mg/ml) was slowly injected over 1 min. In sham-operated animals, rats were injected with an equal volume of saline.

### Drugs and administration

Chronic lumbar intrathecal (i.t.) catheters were implanted using the method described by Storkson.<sup>27</sup> Briefly, under adequate 10% chloral hydrate (330 mg/kg, i.p.) anesthesia, a polyethylene catheter (15 cm, PE-10; RWD,

Shenzhen, China) was introduced into the subarachnoid space via the right L<sub>2/3</sub> intervertebral foramen (removal the facet joint) and advanced carefully 1.5 to 2 cm until it reached the lumbar enlargement. After anesthesia recovery, correct subarachnoid localization of the catheter tip was confirmed by the observation of motor weakness or paralysis induced by 0.1–0.15 ml 2% lidocaine (i.t.). Seven days after implantation, all animals, except those that appeared to have signs of neural dysfunction and infection, were used in experiments. The NF- $\kappa$ B inhibitor PDTC (Sigma, USA) was diluted in sterile NS (final concentration of 0.2 mg/ml) and stored at 4°C. PDTC was administered in a volume of 12  $\mu$ L followed by a flush with 5  $\mu$ L of sterile NS. To observe the cumulative effect, PDTC was injected intrathecally 30 min before the behavior test and then daily thereafter for seven days.

### Behavioral testing

Mechanical allodynia, determined by the paw withdrawal threshold (PWT) in response to von Frey hairs (Stoelting), was tested using the up-down staircase method of Chaplan.<sup>28</sup> In both sham and knee OA rats, behavioral tests were performed one day before injection and on days 7, 14, 21, and 28 postinjection, prior to molecular experiments. Briefly, rats were placed on wire mesh on a shelf and were kept in the apparatus for at least 1 h before the test for acclimation. An ascending series of von Frey filaments was applied to the left and right midplantar regions from below through the mesh to evoke paw withdrawal responses. Each filament was tested five times, and the filament for which three or more paw withdrawal responses out of five tests were elicited was defined as the response threshold. The behavioral testing was conducted by an investigator blinded to the treatment conditions.

### Tissue collection

At the indicated time points before and after injection, the lumbar spinal cord (L<sub>3–5</sub>) was quickly removed under deep anesthesia from half of the rats, and then the tissue samples were dissected and stored in liquid nitrogen. The other half of the rats were terminally anesthetized with 10% chloral hydrate and perfused transcardially with 250 mL room temperature phosphate-buffered saline (PBS) followed by 300 mL ice-cold 4% paraformaldehyde in PBS. The lumbar spinal cord (L<sub>3–5</sub>) was dissected and postfixed in 4% paraformaldehyde overnight, incubated in a sucrose gradient and subsequently sectioned into frozen slices for immunofluorescence. The knee joints were also harvested, and the patella was removed for pathological images. Immediately afterwards, the joints were fixed in 10% formalin and decalcified by immersion in a formic acid solution under constant

agitation at room temperature for five days to produce paraffin slices.

### Histopathology of the knee

Histopathology of the knee was scored based on the recommendations of the Osteoarthritis Research Society International. The severity of cartilage degeneration was scored on a scale of 0–5, with 5 representing the most severe. The osteophyte score was divided into three grades, with 3 representing the presence of large osteophytes. The total joint score was the sum of cartilage degeneration scores at four positions (medial tibial, medial femoral, lateral medial, and lateral tibial) and the osteophyte scores at the medial and lateral positions.

The decalcified tissue was dehydrated, cleared, dipped in wax, embedded, and sliced into 5- $\mu$ m paraffin sections. The sections were double stained with with safranin and fast green. Briefly, the paraffin sections were dewaxed, hydrated in gradient ethanol solutions, double stained with safranin and fast green, dehydrated in gradient alcohol solutions and xylene, and mounted. Images were taken and analysis was performed using an optical microscope (Leica DM4000B) and associated software.

### Western blot assay

The L<sub>3–5</sub> spinal cord segments were removed from liquid nitrogen and ground into a fine powder with a mortar in liquid nitrogen. The powder was homogenized in radio-immunoprecipitation assay buffer containing protease inhibitor phenylmethylsulfonyl fluoride and phosphatase inhibitor (100:1:1). The lysates were then sonicated (six times, 5 s/time, interval: 5 min) and centrifuged (10,600 r/min, 30 min, 4°C). The concentration of the protein extracts was determined with a BCA Protein Assay Kit (Thermo Fisher Scientific). Loading buffer was added to the protein extracts, and the samples were heated at 100°C for 10 min. Then, equivalent amounts of protein (40  $\mu$ g) were separated by 4–12% or 10% NuPAGE Novex Bis-Tris gel (Invitrogen) and transferred to polyvinylidene difluoride membranes (Millipore, USA). The membranes were blocked with 4% BSA for 1 h at room temperature and incubated overnight at 4°C with the following primary antibodies: NF- $\kappa$ B/p65 (1:2000, Abcam, USA), p-p65 (Ser536) (1:1000, Cell Signaling Technology, USA), and  $\beta$ -actin (1:5000, Cell Signaling Technology).

The membranes were washed in Tris-buffered saline containing 0.1% Tween 20 and incubated for 1 h at room temperature with HRP-labeled goat anti-mouse or goat anti-rabbit IgG (1:5000; Cell Signaling Technology). The protein levels were measured by enhanced chemiluminescence (Millipore, USA) and autoradiography. The intensity of the immunoreactive

bands was quantified using Quantity One Analysis Software (version 4.6.5, Bio-Rad Laboratories, USA) and normalized to the density of internal control  $\beta$ -actin.

### Spinal cord immunofluorescence

After postfixation and incubation in gradient sucrose solutions, the L<sub>3-5</sub> segments of the spinal cord were sectioned into 30- $\mu$ m frozen slices according to the method described above. The frozen slices were washed in PBS, and then high-pressure epitope retrieval (2 min) was performed in sodium citrate solution. The sections were incubated for 30 min in PBS containing 1% donkey serum and 0.5% Triton X-100 at 37°C and then incubated overnight at 4°C with a rabbit anti-p-p65 (Ser536) antibody (1:500, Cell Signaling Technology), a mouse anti-GFAP antibody (1:500, Cell Signaling Technology) a mouse anti-NeuN antibody (1:500, Abcam), or a goat anti-IBA-1 antibody (1:500, Abcam). The sections were rinsed in PBS three times for 15 min and then incubated for 30 min at 37°C with corresponding secondary antibodies (conjugated to Alexa FluorVR 488 and 594, Abcam). The samples were finally examined with a Fluorescence Inversion Microscope System (Leica, German), and images were acquired and processed using Leica software.

### RNA extraction and real-time PCR

RNA extraction was performed using the TAKARA RNeasy Kit (TAKARA). After lysis, the samples were incubated with a TAKARA Digestion Kit (TAKARA) to degrade genomic DNA. RNA (1  $\mu$ g) was converted into cDNA (42°C, 5 min) with a TAKARA Reverse Transcription Kit (TAKARA).  $\beta$ -Actin was used as an endogenous control. Total RNA was reverse-transcribed using a reverse transcription system (TAKARA). Real-time polymerase chain reaction (PCR) was performed using SYBR Green (TAKARA) on a Roche instrument. PCR was performed according to the standard protocol (95°C preincubation for 30 s and 95°C incubation for 10 min, followed by 40 cycles of 95°C for 15 s and 60°C for 1 min). Real-time PCR was performed in triplicate, and relative quantification was determined using the relative fold changes by the cycle threshold method (95% confidence interval). All primer sets were subjected to dissociation curve analysis and produced single peaks on a derivative plot of raw fluorescence.

### Statistical analysis

The results are representative of two independent experiments and are presented as the means  $\pm$  standard error of the mean ( $n = 6$  per group in each experiment). One-way analysis of variance (ANOVA) followed by Tukey's  $t$  test was performed to evaluate the differences between

responses. Histopathologic data were analyzed by the Kruskal–Wallis test followed by the Mann–Whitney  $U$  test. Statistical differences were considered to be significant at  $P < 0.05$ .

## Results

### *Intra-articular injection of MIA induced the development of OA in the rat*

**Gross pathology images.** The destruction of the joint significantly increased in the OA group compared with the control group at different time points after the intra-articular injection of MIA (Figure 1(a)).

**Joint space and destruction.** Histopathologic findings were evaluated on days 7, 14, 21, and 28 after MIA injection into the paws of rats with OA. The joint space was significantly decreased, and the destruction of the cartilage and joint structures was significantly increased compared with that of the control group at different time points (overall  $P < 0.01$ ) (Figure 1(b) to (d)). Compared to baseline, no significant difference was found in joint space or histopathologic score on days 7, 14, 21, and 28 following the intra-articular injection of saline (Figure 1(c) and (d),  $P > 0.01$ ). However, compared to baseline, there was a significant difference in joint space on days 7, 14, 21, and 28 following the intra-articular injection of MIA (Figure 1(c),  $P < 0.001$ ). There were significant differences in histopathologic scores on days 7, 14, 21, and 28 following the intra-articular injection of MIA compared to the intra-articular injection of saline (Figure 1(c),  $P < 0.001$ ). The pathological changes in the joints of the knee OA model were basically consistent with knee OA patients.

### *Intra-articular injection of MIA induced a long-lasting increase in NF- $\kappa$ B/p65 in the lumbar spinal dorsal horn and spinally delivered inhibitor PDTC depressed the expression of NF- $\kappa$ B/p65*

Western blotting was performed on the tissue from the lumbar spine dorsal horn on days 0, 7, 14, 21, and 28 following intra-articular injection. No significant difference in the level of NF- $\kappa$ B/p65 protein was found in the saline control group on days 0, 7, 14, 21, and 28 (Figure 2(a) and (b)  $P > 0.05$ ). Compared with control, the intra-articular injection of MIA resulted in an increase in the level of NF- $\kappa$ B/p65 protein on days 7, 14, 21, and 28 (Figure 2(a) and (b),  $P < 0.01$ ). Real-time PCR was also performed to detect the expression of NF- $\kappa$ B/p65 mRNA in the spinal cord. There was no significant difference in the level of NF- $\kappa$ B/p65 mRNA in the saline control group at different time points (Figure 2(c),  $P > 0.01$ ). Compared with rats in the control group,



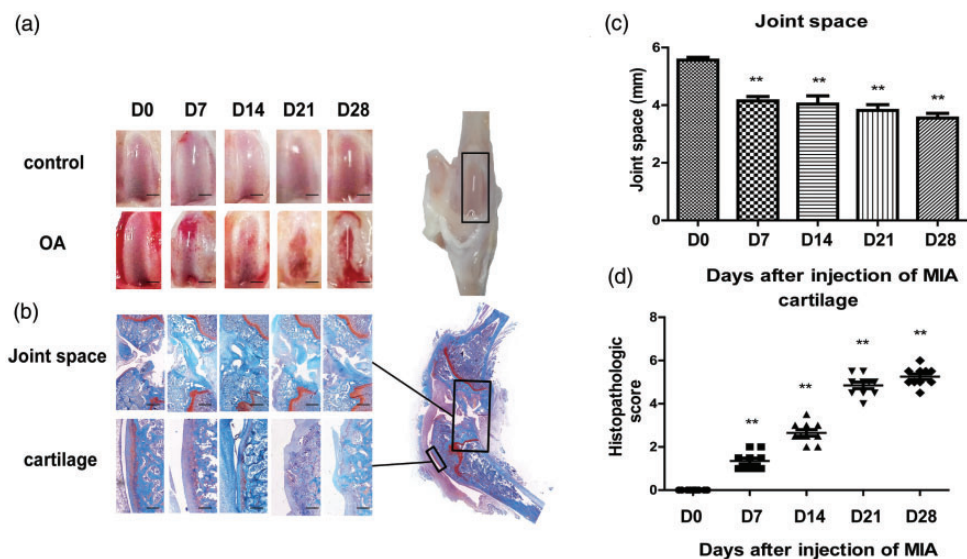


**Figure 1.** Intra-articular injection of monosodium iodoacetate (MIA) induced the development of OA in rats. (a and b) Representative gross photographs of the rat ankle joint and photomicrographs of safranin O/fast green-stained rat ankle joint sections are shown. Bar = 400  $\mu$ m (gross photographs), 400  $\mu$ m (joint space), and 100  $\mu$ m (cartilage). (c) The joint space in rats with OA was measured on days 7, 14, 21, and 28 after the injection of MIA. Day 0 was the time point before MIA injection. (d) Histopathologic scores of OA severity in the rat ankle joint were determined at each time point. The symbols represent the histopathologic scores of individual rats ( $n = 10$  animals/time point). \*\* $P < 0.01$  versus D0 (baseline).

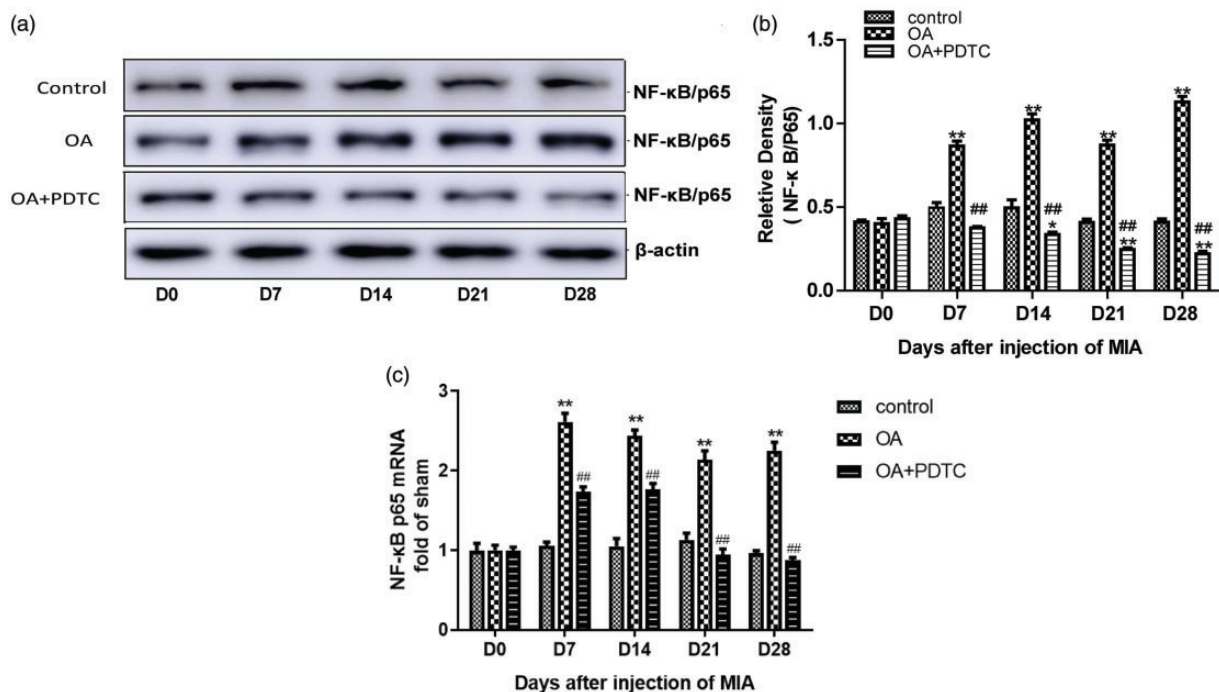


**Figure 2.** Intra-articular injection of MIA induced NF- $\kappa$ B/p65 activation in the spinal cord, and spinally delivered PDTTC inhibited the expression of NF- $\kappa$ B/p65. Rats were treated with saline only (control), MIA alone (OA), or MIA in conjunction with PDTTC after MIA injection (OA+PDTTC). (a) Representative Western blots of NF- $\kappa$ B/p65 expression in rat spinal cord tissue.  $\beta$ -Actin was used as a loading control. (b) Quantitation of the relative densities of the NF- $\kappa$ B/p65 protein bands. The results are expressed as the ratio of NF- $\kappa$ B/p65 to  $\beta$ -actin, and the value at day 0 (D0, baseline) was set at 1.0. (c) Nuclear extracts of spinal cord tissue were evaluated by reverse transcription polymerase chain reaction (real-time PCR) for NF- $\kappa$ B/p65 expression, and the value at day 0 (D0, baseline) was set at 1.0. The results are expressed as the mean  $\pm$  SD of  $n = 5-6$  rats and were analyzed by two-way ANOVA followed by Tukey's  $t$  test. \* $P < 0.05$  versus control; \*\* $P < 0.01$  versus control; # $P < 0.05$  versus OA; ### $P < 0.01$  versus OA.

rats in the MIA group exhibited significantly higher NF- $\kappa$ B/p65 mRNA expression (Figure 2(c),  $P < 0.01$ ). To test the involvement of NF- $\kappa$ B/p65 activation in knee OA, we suppressed NF- $\kappa$ B/p65 activation in the spinal cord by applying the NF- $\kappa$ B family protein inhibitor PDTC via a lumbar subarachnoid catheter. Compared with MIA treatment, the intrathecal injection of PDTC resulted in a trend toward lower expression of NF- $\kappa$ B/p65 protein on days 7, 14, 21, and 28 (Figure 2(a) and (b),  $P < 0.01$ ). Real-time PCR detected that the expression of NF- $\kappa$ B/p65 mRNA in the spinal cord was also decreased compared with that in the MIA group (Figure 2(c),  $P < 0.01$ ). Total NF- $\kappa$ B/p65 at both protein and mRNA levels was upregulated in spinal dorsal horn of OA animals, and the change was depressed by PDTC.

### Level of active p-p65 increased in the lumbar spinal dorsal horn and effects of spinally delivered inhibitor PDTC on the expression of p-p65

P-p65 was also detected in tissue from the lumbar spine dorsal horn on days 0, 7, 14, 21, and 28 following intra-articular injection by Western blotting. No significant difference in the level of p-p65 protein was found in the saline control group on days 0, 7, 14, 21, and 28

(Figure 3(a) and (b)  $P > 0.01$ ). Compared with control, the intra-articular injection of MIA resulted in an increase in the level of p-p65 protein on days 7, 14, 21, and 28 following intra-articular injection (Figure 3(a) and (b),  $P < 0.01$ ). No significant difference in the level of p-p65 protein was found in the saline control group or OA + PDTC group on days 14 and 28 by immunofluorescence of the spinal cord (Figure 4). Level of p-p65 was also upregulated in spinal dorsal horn of OA animals, and the change was depressed by PDTC.

P-p65 was mainly localized in astrocytes, and astrocytes were activated in the lumbar spinal dorsal horn. To determine the main cell type in which p-p65 expression was increased in the lumbar spinal dorsal horn of rats with OA, double staining was performed using anti-p-p65 antibodies and antibodies specific for neurons (NeuN), astrocytes (GFAP), and microglial cells (IBA-1). The fluorescence intensity and quantification revealed that astrocytes were activated in the ipsilateral spinal dorsal horn compared with the contralateral side and that the expression of p-p65 also mainly increased in astrocytes following the intra-articular injection of MIA (Figure 5). There was no significant difference in the number of neurons and microglial cells in the spinal dorsal horn of knee OA model rats. In addition, no

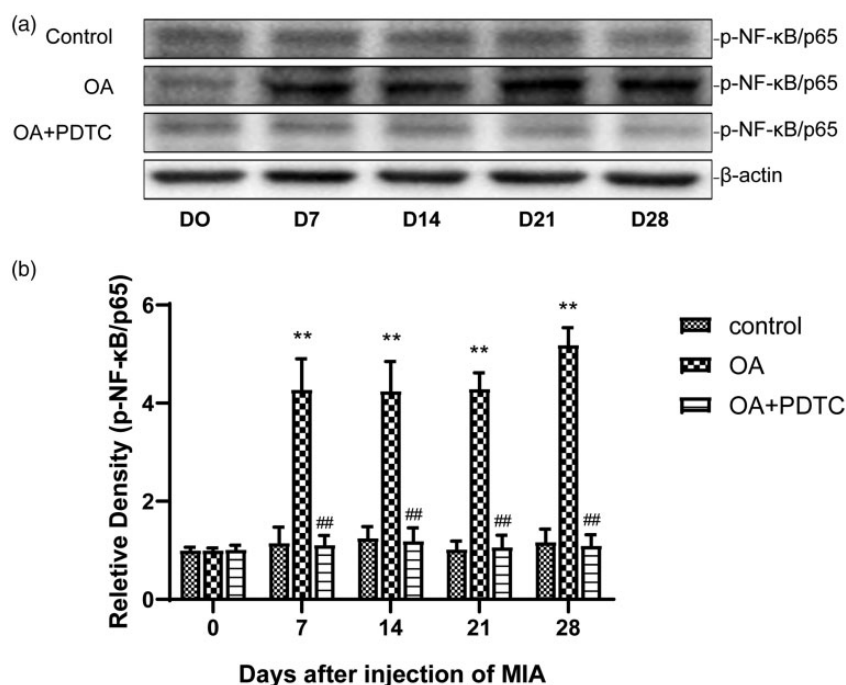


**Figure 3.** Intra-articular injection of MIA induced p-NF- $\kappa$ B/p65 activation in the spinal cord, and spinally delivered PDTC inhibited the expression of p-NF- $\kappa$ B/p65. Rats were treated with saline only (control), MIA alone (OA), or MIA in conjunction with PDTC after MIA injection (OA+PDTC). (a) Representative Western blots of p-NF- $\kappa$ B/p65 expression in rat spinal cord tissue.  $\beta$ -Actin was used as a loading control. (b) Quantitation of the relative densities of the NF- $\kappa$ B/p65 protein bands. The results are expressed as the ratio of p-NF- $\kappa$ B/p65 to  $\beta$ -actin, and the value at day 0 (D0, baseline) was set at 1.0. The results are expressed as the mean  $\pm$  SD of  $n = 5-6$  rats and were analyzed by two-way ANOVA followed by Tukey's  $t$  test. \* $P < 0.05$  versus control; \*\* $P < 0.01$  versus control; # $P < 0.05$  versus OA; ## $P < 0.01$  versus OA.

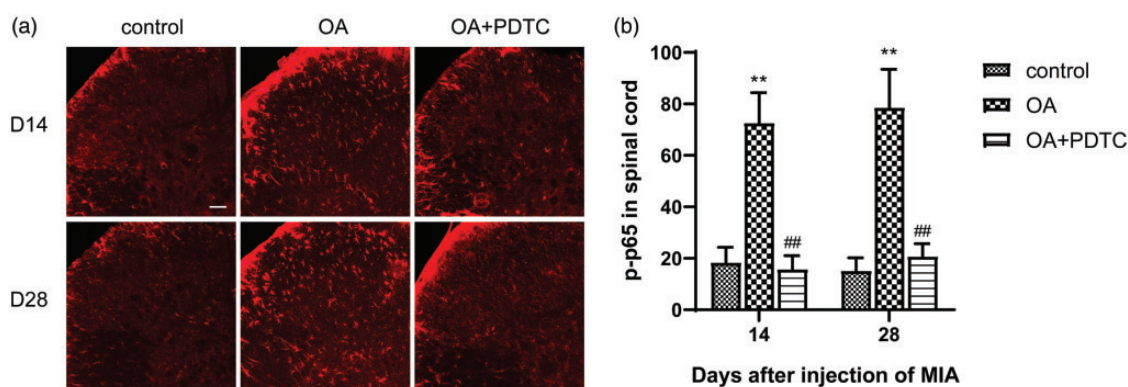


**Figure 4.** Intra-articular injection of MIA induced p-NF-κB/p65 increase in the lumbar spinal dorsal horn. (a) Rats were treated with saline only (control), MIA alone (OA), or MIA in conjunction with PDTC after MIA injection (OA + PDTC). Representative Immunostaining images of p-NF-κB/p65 expression in the spinal dorsal horn on days 14 and 28 after the intra-articular injection of MIA. In panels (a)–(i), bars = 50 μm; (b) Number of cells with high p-NF-κB/p65 expressions. Results are expressed as mean ± SD for n = 5–6 rats and analyzed by two-way ANOVA followed by Tukey's *t* test. \**P* < 0.05 versus control; \*\**P* < 0.01 versus control; ##*P* < 0.05 versus OA; ###*P* < 0.01 versus OA.

significant difference of p-p65 in neurons and microglial cells was found between the ipsilateral and contralateral sides of the lumbar spinal dorsal horn of knee OA model rats. Results of immunofluorescence revealed that astrocytes were activated and that p-p65 was mainly increased in astrocytes in spinal dorsal horn of OA animals.

#### Effects of spinally delivered NF-κB/p65 inhibitor PDTC on mechanical hyperalgesia

No significant differences in baseline mechanical threshold values were found in either group (knee OA model rats and saline controls) or among the groups. The intra-articular injection of saline resulted in no change in mechanical hyperalgesia (*P* > 0.5), but the intra-articular injection of MIA resulted in a decrease in mechanical threshold on days 7, 14, 21, and 28 (Figure 6, *P* < 0.01). Compared with that of the saline group, the mechanical threshold was decreased on days 7, 14, 21, and 28 (Figure 6, *P* < 0.01). The overall trend of hyperalgesia was that it first increased and was then maintained at a higher level, which is basically consistent with the clinical characteristics of OA patients. Moreover, the mechanical hyperalgesia of the animals in the PDTC groups was significantly higher than that of the animals in the MIA group from day 21 to day 28 (Figure 6, *P* < 0.01). The intrathecal injection of PDTC markedly prevented the MIA-induced reduction in the PWT.

#### Effects of spinally delivered NF-κB/p65 inhibitor PDTC on the expression of IL-1β, TNF-α, and IL-33

The results indicated that the expression levels of IL-1β, TNF-α, and IL-33 were significantly increased in the MIA group compared with the control group (all *P* values < 0.01). In addition, the TNF-α and IL-33

mRNA levels in the PDTC group were significantly lower than those in the MIA group on days 14 and 28 (Figure 7(a) and (b), all *P* values < 0.01). However, the expression of IL-1β was modestly, but not significantly, lower in the PDTC group than in the MIA group (Figure 7(c), all *P* values > 0.01). Furthermore, the expression of the IL-1β gene in the MIA group was also obviously lower than that in the PDTC group (Figure 5(c), all *P* values < 0.01). Intrathecal injection of PDTC markedly depressed the upregulation of pain-related inflammatory factor in spinal dorsal horn of OA animals.

## Discussion

The underlying mechanism of advanced knee OA is complex and unclear. A growing number of studies have revealed that central sensitization, not only peripheral changes, participates in advanced knee OA pain. Our results demonstrated that MIA induced the typical pathological changes and hyperalgesia in the advanced knee OA model and increased the expression of NF-κB/p65, p-p65 and cytokines (IL-1β, TNF-α and IL-33) in the spinal cord. Furthermore, the NF-κB/p65 inhibitor PDTC reduces hyperalgesia and the upregulation of IL-1β, TNF-α, and IL-33.

Knee OA pain continued to increase in the early stage and was then maintained at a higher level. The hyperalgesic behaviors of the knee OA model rats were basically consistent with the clinical characteristics of OA patients.<sup>29</sup> MIA intra-articular injection, which is simple and quick, is a well-accepted method to establish a knee OA model. Nevertheless, there are still some differences in the dose of MIA used. In our study, we chose a higher dose of MIA to establish an advanced knee OA



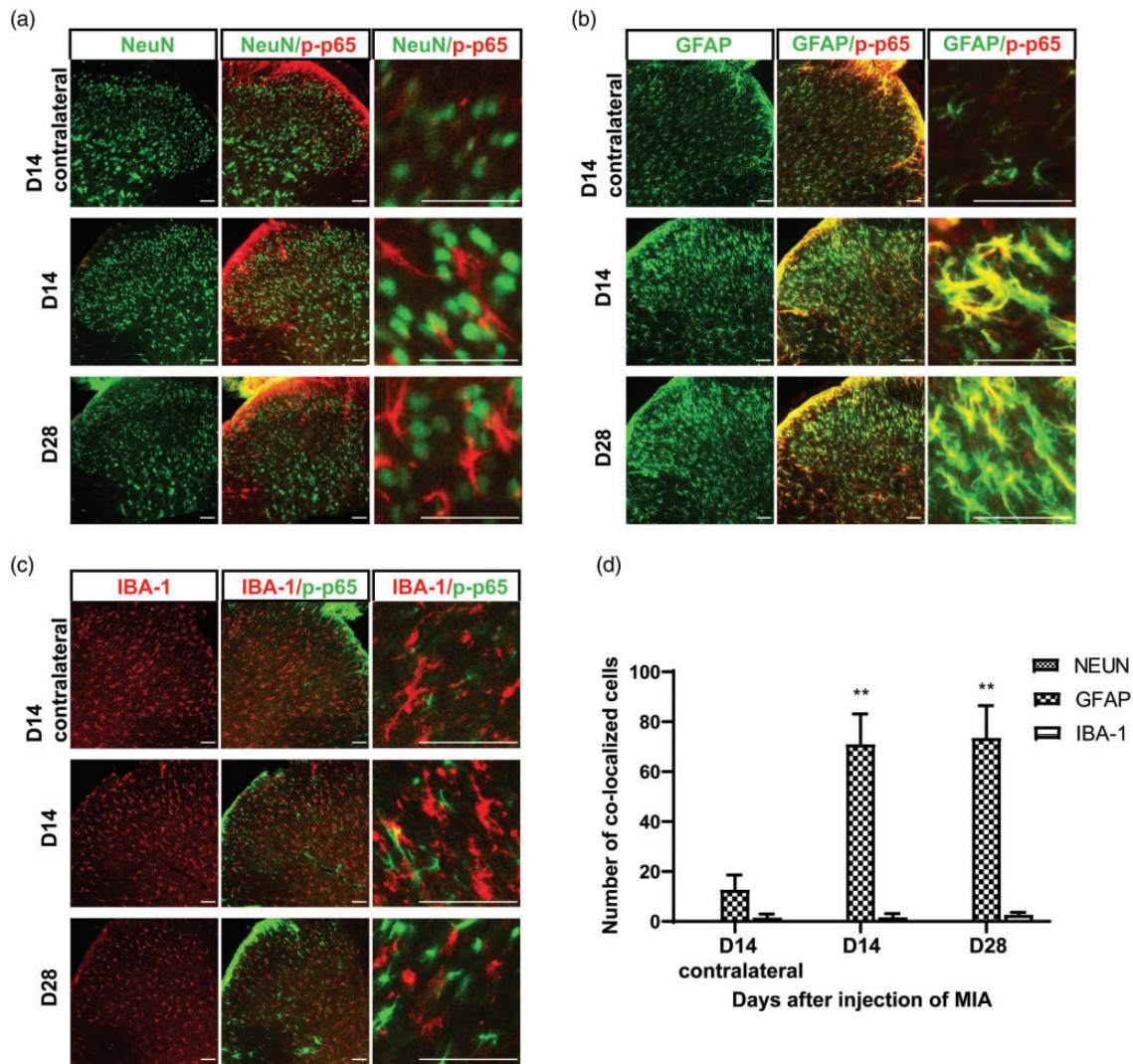


**Figure 5.** The expression of p-p65 in different cell types induced by intra-articular injection of MIA in the lumbar spinal dorsal horn. Representative immunostaining images of NeuN-immunoreactive neurons (a), glial fibrillary acidic protein (GFAP)-immunoreactive astrocytes (b), IBA-1-immunoreactive microglial cells (c) and the co-locations with p-p65 in the spinal dorsal horn on day 14 (ipsilateral and contralateral) and day 28 after the intra-articular injection of MIA. Scale bar = 50  $\mu$ m. (d) Number of cells with high p-p65 expressions. Results are expressed as mean  $\pm$  SD for  $n = 5-6$  rats and analyzed by one-way ANOVA followed by Tukey's  $t$  test. \* $P < 0.05$  versus control; \*\* $P < 0.01$  versus control.

model, which has been confirmed to manifest as spontaneous pain that cannot be relieved by the common NSAIDs.<sup>7,30</sup> Our results confirmed that the MIA model displayed histologic features similar to the clinical features of OA (destruction of cartilage articular subchondral bone, joint space, etc.). During the development of experimental knee OA, continuous and intense nociceptive input from the joint may induce complex changes in the central nervous system (central sensitization).<sup>10</sup> Cytokines and chemokines have been demonstrated to be involved in the induction and maintenance of central sensitization, and they are possible mediators of widespread central sensitization.<sup>31</sup> TNF- $\alpha$  also inhibits

the spontaneous action potentials of GABAergic neurons in the dorsal horn.<sup>32</sup> It has been found that IL-1 $\beta$  regulates central sensitization by increasing glutamate release, increasing the phosphorylation of NMDA receptors,<sup>33,34</sup> and potentiating presynaptic NMDA receptor function in neuropathic pain.<sup>35</sup> It is well demonstrated that the spinal content of cytokines, including IL-1 $\beta$  and other inflammatory mediators are enhanced in the lumbar spinal cord of MIA-induced OA models.<sup>15,36</sup> Significantly elevated concentrations of TNF- $\alpha$  and higher expression of CGRP have also been confirmed in the MIA model.<sup>37</sup> Consistent with this study, we found that the expression levels of TNF- $\alpha$ , IL-1 $\beta$ , and IL-33 protein were highly



upregulated in the spinal cord of the advanced knee OA model.

As inflammatory factors in the central nervous system have been confirmed to promote hyperalgesia in advanced OA, inhibiting central inflammatory factors and alleviating hyperalgesia have attracted increasing attention. The blockade of IL-6 function by tocilizumab significantly mitigates mechanical allodynia in rats with

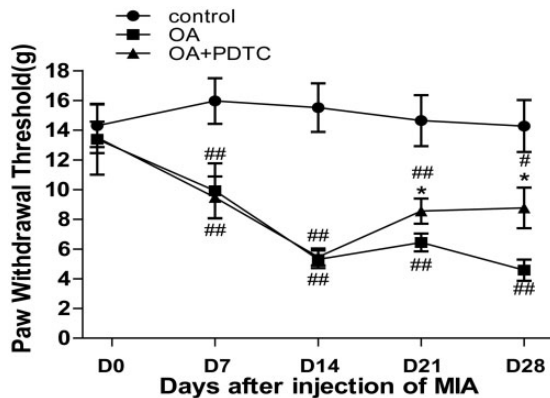


**Figure 6.** Analgesic effects of spinally delivered NF- $\kappa$ B/p65 inhibitor PDTC in rats with OA. The paw withdrawal thresholds were measured on days 7, 14, 21, and 28 after the intra-articular injection of MIA. Day 0 was the time point before MIA injection. The results are expressed as the mean  $\pm$  SD of  $n = 5-6$  rats and were analyzed by two-way ANOVA followed by Tukey's  $t$  test. # $P < 0.05$  versus vehicle; ## $P < 0.01$  versus vehicle; \* $P < 0.05$  versus OA; \*\* $P < 0.01$  versus OA.

MIA-induced OA.<sup>38</sup> It is well documented that spinal cord-specific cytokines, such as IL-1 $\beta$ , TNF $\alpha$ , and IL-6, and neuropeptides can be regulated by NF- $\kappa$ B.<sup>39,40</sup> NF- $\kappa$ B, a key transcription factor, plays a fundamental role in inflammatory diseases, including autoimmune disorders, cancer, and neurodegeneration. The activation of NF- $\kappa$ B in response to peripheral nerve injury or tissue inflammation can increase inflammatory factors and induce refractory pain and neuropathic pain.<sup>41</sup> Spinal NF- $\kappa$ B activation induces spinal TNF- $\alpha$ , IL-1 $\beta$ , and COX-2 upregulation and pain hypersensitivity following peripheral inflammation.<sup>25,42</sup> In a chronic constriction injury (CCI) model, the suppression of NF- $\kappa$ B/p65 alleviates mechanical allodynia by inhibiting the upregulation of proinflammatory factors (TNF- $\alpha$ , IL-1 $\beta$ , and IL-6) in the spinal cord.<sup>24</sup> IL-33-induced hyperalgesia in the CCI model is markedly attenuated by an NF- $\kappa$ B inhibitor and inhibits IL-33-induced TNF- $\alpha$  and IL-1 $\beta$  production in the spinal cord.<sup>43</sup> In addition, minocycline significantly reverses bone cancer pain-induced mechanical tactile allodynia by inhibiting the translocation of NF- $\kappa$ B to the nucleus in IL-1 $\beta$ -stimulated primary rat astrocytes.<sup>44</sup> Consistent with these studies, our present results showed that the intra-articular injection of MIA significantly decreased the ipsilateral pain threshold and increased spinal NF- $\kappa$ B/p65 and that spinally delivered NF- $\kappa$ B/p65 inhibitor PDTC obviously attenuated hyperalgesia in the advanced knee OA model. In addition, our results demonstrated that spinally delivered NF- $\kappa$ B/p65

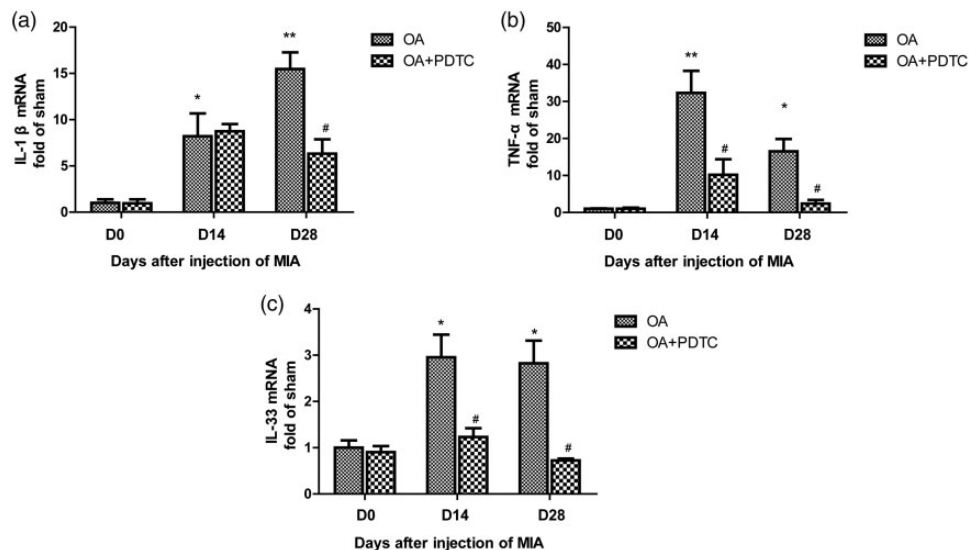


**Figure 7.** Effects of the intrathecal injection of the NF- $\kappa$ B/p65 inhibitor PDTC on the expression of spinal IL-1 $\beta$ , TNF- $\alpha$ , and IL-33. The expression levels of spinal IL-1 $\beta$  (A), TNF- $\alpha$  (B), and IL-33 (C) in each treatment group were detected at the mRNA level by real-time PCR on days 0, 14, 28 after the intra-articular injection of MIA. The results are expressed as the mean  $\pm$  SD of  $n = 5-6$  rats and were analyzed by one-way ANOVA and two-way ANOVA followed by Tukey's  $t$  test. \* $P < 0.05$  versus D0; # $P < 0.05$  versus OA.

inhibitor PDTC markedly reduced the spinal overexpression of TNF- $\alpha$ , IL-1 $\beta$ , and IL-33 proteins and alleviated hyperalgesia. These results suggested that the activation of NF- $\kappa$ B/p65 in the spinal cord induced upregulation of inflammatory mediators, such as TNF- $\alpha$ , IL-1 $\beta$ , and IL-33, which may contribute to the underlying mechanism of advanced knee OA.

Studies have found that NF- $\kappa$ B activity is an additional layer of complexity imposed by posttranslational modifications of NF- $\kappa$ B and their regulators.<sup>45</sup> Recently, it was confirmed that the activation of NF- $\kappa$ B-dependent transcription is mediated by the phosphorylation of NF- $\kappa$ B/p65 in many inflammatory diseases.<sup>21</sup> It has been found that spinal nerve ligation induces neuropathic pain by promoting the phosphorylation of NF- $\kappa$ B/p65 and resulting in the upregulation of its downstream target genes, such as TNF- $\alpha$ , IL-1 $\beta$ , and IL-6.<sup>46</sup> Similarly, our data supported that p-p65 increased the protein levels of proinflammatory cytokines and induced the generation of pain. Importantly, it is also becoming apparent that certain forms of p-p65 may either enhance or downregulate the transcription of select target genes in a gene-specific manner rather than acting as a simple on/off switch. It is of interest to understand such gene-specific regulatory processes that may selectively modulate NF- $\kappa$ B activity for their potential therapeutic benefits. Further study is needed to evaluate the selective modulation of NF- $\kappa$ B.

A large number of studies have proved that the occurrence and development of chronic pain is accompanied by the activation of astrocytes in the spinal dorsal horn of various animal models of pain.<sup>47</sup> In a rat neuropathic pain model, microglia are activated in the early stages of pain, and astrocytes are significantly important in the process of persistent pain.<sup>48</sup> Astrocyte activation can last three to five months, and the degree of activation is linearly related to pain behavior; the intrathecal injection of astrocyte inhibitors significantly ameliorates the established mechanical hyperalgesia.<sup>49</sup> Interestingly, previous studies have shown that astrocytic NF- $\kappa$ B activity drives the extent of hyperalgesia and allodynia in different chronic pain models,<sup>50–52</sup> which suggests a role for NF- $\kappa$ B in the modulation of astrocytes to facilitate the generation of chronic pain. Our study found that the number of astrocytes increased significantly in a rat model of advanced knee OA and that the level of p-p65 in astrocytes increased significantly. Therefore, we speculate that NF- $\kappa$ B in astrocytes plays a critical role in advanced knee OA pain. There are also some limitations to our research. The specific mechanism of astrocyte activation induced by NF- $\kappa$ B and how astrocyte activation leads to pain after activation in the spinal cord of OA model rats requires further study.

In conclusion, our findings indicate a pivotal role for spinal NF- $\kappa$ B/p65 in the underlying mechanism of

advanced knee OA pain. Inhibiting the expression of spinal NF- $\kappa$ B/p65 markedly reduced advanced knee OA pain. Thus, targeting spinal NF- $\kappa$ B/p65 may provide a novel treatment option for painful inflammatory disorders, including advanced knee OA.

### Declaration of Conflicting Interests


The author(s) declared no potential conflicts of interest with respect to the research, authorship, and/or publication of this article.

### Funding

The author(s) disclosed receipt of the following financial support for the research, authorship, and/or publication of this article: This research was supported by grants from the National Natural Science Foundation of China (No. 81300964), the China Postdoctoral Science Foundation (No. 2014M551922, No. 2013M531611, and No. 2014T70648), and the Natural Science Foundation of Shandong Province (No. ZR2014HQ041 and No. ZR2009CQ016) and Foundation for Outstanding Young Scientist in Shandong Province grant No. BS2013YY047.

### ORCID iDs

Yunze Li  <https://orcid.org/0000-0001-9269-5644>

Zhiying Feng  <https://orcid.org/0000-0003-0962-9449>

### References

1. Neogi T. The epidemiology and impact of pain in osteoarthritis. *Osteoarthr Cartil* 2013; 21: 1145–1153.
2. Cross M, Smith E, Hoy D, Nolte S, Ackerman I, Fransen M, Bridgett L, Williams S, Guillemin F, Hill CL, Laslett LL, Jones G, Cicuttini FM, Osborne R, Vos T, Buchbinder R, Woolf A, March L. The global burden of hip and knee osteoarthritis: estimates from the Global Burden of Disease 2010 study. *Ann Rheum Dis* 2014; 73: 1323–1330.
3. Tang X, Wang S, Zhan S, Niu J, Tao K, Zhang Y, Lin J. The prevalence of symptomatic knee osteoarthritis in china results from the China health and retirement longitudinal study. *Arthritis Rheumatol* 2016; 68: 648–653.
4. Schaible H-G. Mechanisms of chronic pain in osteoarthritis. *Curr Rheumatol Rep* 2012; 14: 549–556.
5. Beswick AD, Wylde V, Gooberman-Hill R, Blom A, Dieppe P. What proportion of patients report long-term pain after total hip or knee replacement for osteoarthritis? A systematic review of prospective studies in unselected patients. *BMJ Open* 2012; 2: e000435.
6. Hawker GA, Stewart L, French MR, Cibere J, Jordan JM, March L, Suarez-Almazor M, Gooberman-Hill R. Understanding the pain experience in hip and knee osteoarthritis—an OARSI/OMERACT initiative. *Osteoarthr Cartil* 2008; 16: 415–422.
7. Havelin J, Imbert I, Cormier J, Allen J, Porreca F, King T. Central sensitization and neuropathic features of ongoing pain in a rat model of advanced osteoarthritis. *J Pain* 2016; 17: 374–382.

8. Suokas AK, Walsh DA, McWilliams DF, Condon L, Moreton B, Wylde V, Arendt-Nielsen L, Zhang W. Quantitative sensory testing in painful osteoarthritis: a systematic review and meta-analysis. *Osteoarthr Cartil* 2012; 20: 1075–1085.
9. Rahman W, Bauer CS, Bannister K, Vonsy J-L, Dolphin AC, Dickenson AH. Descending serotonergic facilitation and the antinociceptive effects of pregabalin in a rat model of osteoarthritic pain. *Mol Pain* 2009; 5: 1744–8069.
10. Sagar DR, Staniaszek LE, Okine BN, Woodhams S, Norris LM, Pearson RG, Garle MJ, Alexander SPH, Bennett AJ, Barrett DA, Kendall DA, Scammell BE, Chapman V. Tonic modulation of spinal hyperexcitability by the endocannabinoid receptor system in a rat model of osteoarthritis pain. *Arthritis Rheum* 2010; 62: 3666–3676.
11. Eitner A, Hofmann GO, Schaible H-G. Mechanisms of osteoarthritic pain. studies in humans and experimental models. *Front Mol Neurosci* 2017; 10: 349.
12. Konttinen YT, Sillat T, Barreto G, Ainola M, Nordstrom D. Osteoarthritis as an autoinflammatory disease caused by chondrocyte-mediated inflammatory responses. *Arthritis Rheum* 2012; 64: 613–616.
13. Harkey MS, Luc BA, Golightly YM, Thomas AC, Driban JB, Hackney AC, Pietrosimone B. Osteoarthritis-related biomarkers following anterior cruciate ligament injury and reconstruction: a systematic review. *Osteoarthr Cartil* 2015; 23: 1–12.
14. Larsson S, Englund M, Struglics A, Lohmander LS. Interleukin-6 and tumor necrosis factor alpha in synovial fluid are associated with progression of radiographic knee osteoarthritis in subjects with previous meniscectomy. *Osteoarthr Cartil* 2015; 23: 1906–1914.
15. Im HJ, Kim JS, Li X, Kotwal N, Sumner DR, van Wijnen AJ, Davis FJ, Yan D, Levine B, Henry JL, Desevré J, Kroin JS. Alteration of sensory neurons and spinal response to an experimental osteoarthritis pain model. *Arthritis Rheum* 2010; 62: 2995–3005.
16. Ji RR, Nackley A, Huh Y, Terrando N, Maixner W. Neuroinflammation and central sensitization in chronic and widespread pain. *Anesthesiology* 2018; 129: 343–366.
17. Niederberger E, Geisslinger G. The IKK-NF-kappaB pathway: a source for novel molecular drug targets in pain therapy? *Faseb J* 2008; 22: 3432–3442.
18. Li D, Huang Z-Z, Ling Y-Z, Wei J-Y, Cui Y, Zhang X-Z, Zhu H-Q, Xin W-J. Up-regulation of CX3CL1 via nuclear factor-kappa B-dependent histone acetylation is involved in paclitaxel-induced peripheral neuropathy. *Anesthesiology* 2015; 122: 1142–1151.
19. Tegeder I, Niederberger E, Schmidt R, Kunz S, Guhring H, Ritzeler O, Michaelis M, Geisslinger G. Specific inhibition of IkappaB kinase reduces hyperalgesia in inflammatory and neuropathic pain models in rats. *J Neurosci* 2004; 24: 1637–1645.
20. Herkenham M, Rathore P, Brown P, Listwak SJ. Cautionary notes on the use of NF-kappa B p65 and p50 antibodies for CNS studies. *J Neuroinflamm* 2011; 8: 141.
21. Christian F, Smith EL, Carmody RJ. The regulation of NF-kappa B subunits by phosphorylation. *Cells*. 2016; 5: 12.
22. Chen LF, Williams SA, Mu YJ, Nakano H, Duerr JM, Buckbinder L, Greene WC. NF-kappa B RelA phosphorylation regulates RelA acetylation. *Mol Cell Biol* 2005; 25: 7966–7975.
23. Dong J, Jimi E, Zhong H, Hayden MS, Ghosh S. Repression of gene expression by unphosphorylated NF-kappa B p65 through epigenetic mechanisms. *Genes Dev* 2008; 22: 1159–1173.
24. Sun T, Luo J, Jia M, Li H, Li K, Fu Z. Small interfering RNA-mediated knockdown of NF-kBp65 attenuates neuropathic pain following peripheral nerve injury in rats. *Eur J Pharmacol* 2012; 682: 79–85.
25. Luo JG, Zhao XL, Xu WC, Zhao XJ, Wang JN, Lin XW, Sun T, Fu ZJ. Activation of spinal NF-kB/p65 contributes to peripheral inflammation and hyperalgesia in rat adjuvant-induced arthritis. *Arthritis Rheumatol* 2014; 66: 896–906.
26. Guzman RE, Evans MG, Bove S, Morenko B, Kilgore K. Mono-iodoacetate-induced histologic changes in subchondral bone and articular cartilage of rat femorotibial joints: an animal model of osteoarthritis. *Toxicol Pathol* 2003; 31: 619–624.
27. Storkson RV, Kjorsvik A, Tjolsen A, Hole K. Lumbar catheterization of the spinal subarachnoid space in the rat. *J Neurosci Methods* 1996; 65: 167–172.
28. Chaplan SR, Bach FW, Pogrel JW, Chung JM, Yaksh TL. Quantitative assessment of tactile allodynia in the rat paw. *J Neurosci Methods* 1994; 53: 55–63.
29. Thakur M, Dickenson AH, Baron R. Osteoarthritis pain: nociceptive or neuropathic? *Nat Rev Rheumatol* 2014; 10: 374–380.
30. Liu P, Okun A, Ren J, Guo RC, Ossipov MH, Xie J, King T, Porreca F. Ongoing pain in the MIA model of osteoarthritis. *Neurosci Lett* 2011; 493: 72–75.
31. Kawasaki Y, Zhang L, Cheng J-K, Ji R-R. Cytokine mechanisms of central sensitization: distinct and overlapping role of interleukin-1 beta, interleukin-6, and tumor necrosis factor-beta in regulating synaptic and neuronal activity in the superficial spinal cord. *J Neurosci* 2008; 28: 5189–5194.
32. Zhang H, Nie H, Dougherty PM. A p38 mitogen-activated protein kinase-dependent mechanism of disinhibition in spinal synaptic transmission induced by tumor necrosis factor-alpha. *J Neurosci* 2010; 30: 12844–12855.
33. Guo W, Wang H, Watanabe M, Shimizu K, Zou S, LaGraize SC, Wei F, Dubner R, Ren K. Glial-cytokine-neuronal interactions underlying the mechanisms of persistent pain. *J Neurosci* 2007; 27: 6006–6018.
34. Zhang R-X, Li A, Liu B, Wang L, Ren K, Zhang H, Berman BM, Lao L. IL-1ra alleviates inflammatory hyperalgesia through preventing phosphorylation of NMDA receptor NR-1 subunit in rats. *Pain* 2008; 135: 232–239.
35. Yan X, Weng H-R. Endogenous interleukin-1 beta in neuropathic rats enhances glutamate release from the primary afferents in the spinal dorsal horn through coupling with presynaptic N-Methyl-D-aspartic acid receptors. *J Biol Chem* 2013; 288: 30544–30557.
36. Lockwood SM, Lopes DM, McMahon SB, Dickenson AH. Characterisation of peripheral and central components of the



- rat monoiodoacetate model of Osteoarthritis. *Osteoarthr Cartil* 2019; 27: 712–722.
37. Kawarai Y, Orita S, Nakamura J, Miyamoto S, Suzuki M, Inage K, Hagiwara S, Suzuki T, Nakajima T, Akazawa T, Ohtori S. Changes in proinflammatory cytokines, neuropeptides, and microglia in an animal model of monosodium iodoacetate-induced hip osteoarthritis. *J Orthop Res* 2018; 36: 2978–2986.
  38. Lin Y, Liu L, Jiang H, Zhou J, Tang Y. Inhibition of interleukin-6 function attenuates the central sensitization and pain behavior induced by osteoarthritis. *Eur J Pharmacol* 2017; 811: 260–267.
  39. Chiechio S, Zammataro M, Morales ME, Busceti CL, Drago F, Gereau RWI, Copani A, Nicoletti F. Epigenetic modulation of mGlu2 receptors by histone deacetylase inhibitors in the treatment of inflammatory pain. *Mol Pharmacol* 2009; 75: 1014–1020.
  40. Ahmed AS, Ahmed M, Li J, Gu HF, Bakalkin G, Stark A, Harris HE. Proteasome inhibitor MG132 modulates inflammatory pain by central mechanisms in adjuvant arthritis. *Int J Rheum Dis* 2017; 20: 25–32.
  41. Fu ES, Zhang YP, Sagen J, Candiotti KA, Morton PD, Liebl DJ, Bethea JR, Brambilla R. Transgenic inhibition of glial NF-kappa B reduces pain behavior and inflammation after peripheral nerve injury. *Pain* 2010; 148: 509–518.
  42. Lee KM, Kang BS, Lee HL, Son SJ, Hwang SH, Kim DS, Park JS, Cho HJ. Spinal NF-kB activation induces COX-2 upregulation and contributes to inflammatory pain hypersensitivity. *Eur J Neurosci* 2004; 19: 3375–3381.
  43. Zarpelon AC, Rodrigues FC, Lopes AH, Souza GR, Carvalho TT, Pinto LG, Xu D, Ferreira SH, Alves-Filho JC, McInnes IB, Ryffel B, Quesniaux VFJ, Reverchon F, Mortaud S, Menuet A, Liew FY, Cunha FQ, Cunha TM, Verri WA. Jr., Spinal cord oligodendrocyte-derived alarmin IL-33 mediates neuropathic pain. *Faseb J* 2016; 30: 54–65.
  44. Song Z-P, Xiong B-R, Guan X-H, Cao F, Manyande A, Zhou Y-Q, Zheng H, Tian Y-K. Minocycline attenuates bone cancer pain in rats by inhibiting NF-kappa B in spinal astrocytes. *Acta Pharmacol Sin* 2016; 37: 753–762.
  45. Colleran A, Collins PE, O'Carroll C, Ahmed A, Mao X, McManus B, Kiely PA, Burstein E, Carmody RJ. Deubiquitination of NF-kappa B by ubiquitin-specific protease-7 promotes transcription. *Proc Natl Acad Sci USA* 2013; 110: 618–623.
  46. Gao J, Tang C, Tai LW, Ouyang Y, Li N, Hu Z, Chen X. Pro-resolving mediator maresin 1 ameliorates pain hypersensitivity in a rat spinal nerve ligation model of neuropathic pain. *J Pain Res* 2018; 11: 1511–1519.
  47. Old EA, Clark AK, Malcangio M. The role of glia in the spinal cord in neuropathic and inflammatory pain. *Handb Exp Pharmacol* 2015; 227: 145–170.
  48. Popiolek-Barczyk K, Mika J. Targeting the microglial signaling pathways: new insights in the modulation of neuropathic pain. *Curr Med Chem* 2016; 23: 2908–2928.
  49. Chiang C-Y, Wang J, Xie Y-F, Zhang S, Hu JW, Dostrovsky JO, Sessle BJ. Astroglial glutamate-glutamine shuttle is involved in central sensitization of nociceptive neurons in rat medullary dorsal horn. *J Neurosci* 2007; 27: 9068–9076.
  50. Hartung JE, Eskew O, Wong T, Tchivileva IE, Olatosu FA, O'Buckley SC, Nackley AG. Nuclear factor-kappa B regulates pain and COMT expression in a rodent model of inflammation. *Brain Behav Immun* 2015; 50: 196–202.
  51. Xu J, Zhu MD, Zhang X, Tian H, Zhang JH, Wu XB, Gao YJ. NF-kB-mediated CXCL1 production in spinal cord astrocytes contributes to the maintenance of bone cancer pain in mice. *J Neuroinflammation* 2014; 11: 38.
  52. Zhou L, Hu Y, Li C, Yan Y, Ao L, Yu B, Fang W, Liu J, Li Y. Levo-corydalmine alleviates vincristine-induced neuropathic pain in mice by inhibiting an NF-kappa B-dependent CXCL1/CXCR2 signaling pathway. *Neuropharmacology* 2018; 135: 34–47.